Molecular Cancer Research

Hyperactivation of MAPK Signaling Is Deleterious to RAS/RAF-mutant Melanoma

Grace P. Leung[1], Tianshu Feng[1], Frederic D. Sigoillot[2], Felipe C. Geyer[1], Matthew D. Shirley[1], David A. Ruddy[1], Daniel P. Rakiec[1], Alyson K. Freeman[1], Jeffrey A. Engelman[1], Mariela Jaskelioff[1], and Darrin D. Stuart[1]

Abstract

The most frequent genetic alterations in melanoma are gain-of-function (GOF) mutations in BRAF, which result in RAF–MEK–ERK signaling pathway addiction. Despite therapeutic success of RAF and MEK inhibitors in treating $BRAF^{V600}$-mutant tumors, a major challenge is the inevitable emergence of drug resistance, which often involves reactivation of the MAPK pathway. Interestingly, resistant tumors are often sensitive to drug withdrawal, suggesting that hyperactivation of the MAPK pathway is not tolerated. To further characterize this phenomenon, isogenic models of inducible MAPK hyperactivation in $BRAF^{V600E}$ melanoma cells were generated by overexpression of ERK2. Using this model system, supraphysiologic levels of MAPK signaling led to cell death, which was reversed by MAPK inhibition. Furthermore, complete tumor regression was observed in an ERK2-overexpressing xenograft model. To identify mediators of MAPK hyperactivation–induced cell death, a large-scale pooled shRNA screen was conducted, which revealed that only shRNAs against *BRAF* and *MAP2K1* rescued loss of cell viability. This suggested that no single downstream ERK2 effector was required, consistent with pleiotropic effects on multiple cellular stress pathways. Intriguingly, the detrimental effect of MAPK hyperactivation could be partially attributed to secreted factors, and more than 100 differentially secreted proteins were identified. The effect of ERK2 overexpression was highly context dependent, as RAS/RAF mutant but not RAS/RAF wild-type melanoma were sensitive to this perturbation.

Implications: This vulnerability to MAPK hyperactivation raises the possibility of novel therapeutic approaches for RAS/RAF-mutant cancers.

Introduction

The MAPK signaling pathway, comprised of RAS, RAF, MEK and ERK, is involved in transduction of extracellular nutrient and growth factor signals to the interior of the cell. As such, it regulates a large number of cell processes including cell proliferation, differentiation, and survival. Because of its critical role in cell growth, MAPK pathway genes are frequently mutated in cancer. Fifty percent of all metastatic melanoma tumors harbor $BRAF^{V600}$ mutations, which lead to elevated MAPK pathway signaling and promote tumor growth (1–3). These tumors exhibit exquisite dependence upon mutant BRAF for survival, making BRAF an attractive target for pharmacologic intervention. Indeed, RAF inhibitors such as vemurafenib and dabrafenib have been successful in improving progression-free and overall survival of patients with metastatic melanoma harboring BRAF V600 mutations (4, 5). However, resistance to inhibitors invariably develops, frequently attained via upregulation of the MAPK pathway through NRAS, KRAS, or MEK mutations (6–11), and amplification or alternative splicing of BRAF (9, 12–14).

We and others have reported that tumors that develop resistance to MAPK inhibitors become addicted to the drug, in that drug withdrawal leads to inhibition of cell proliferation *in vitro* and *in vivo* (15–18). This was shown to be due to hyperactivation of MAPK signaling, which confers a benefit during pathway inhibition induced by drug treatment, but comes with a fitness cost in the absence of drug. These observations suggest that cells must maintain a finely tuned level of MAPK signaling, which drives tumor growth within a limited range, but is not tolerated above a certain threshold.

To further characterize the molecular underpinnings of this phenomenon, we generated isogenic models of inducible MAPK hyperactivation in $BRAF^{V600E}$ melanoma cells by overexpressing ectopic ERK2. In contrast to the cell stasis observed after treatment with MAPK inhibitors, hyperactive MAPK signaling due to ERK2 overexpression led to cell death. This response was specific to MAPK pathway hyperactivation, as the effects could be abrogated by MAPK inhibitors. Furthermore, a pooled shRNA screen identified shRNAs targeting *BRAF* and *MAP2K1* as rescuers of ERK2 overexpression–induced cell death. We sought to describe the stress responses and cell death pathways induced in this system. Surprisingly, we discovered that secreted factors contributed to the deleterious effects of MAPK hyperactivation. The ERK2 overexpression–induced cell death observed *in vitro* translated to an *in vivo* xenograft model, which showed complete tumor regression. ERK2 overexpression resulted in reduced viability only in RAS/RAF-mutated melanoma cell lines, but had no effect on RAS/RAF

[1]Oncology, Novartis Institutes for BioMedical Research, Cambridge, Massachusetts. [2]Chemical Biology and Therapeutics, Novartis Institutes for BioMedical Research, Cambridge, Massachusetts.

Note: Supplementary data for this article are available at Molecular Cancer Research Online (http://mcr.aacrjournals.org/).

Corresponding Authors: Darrin D. Stuart, Novartis Institutes for BioMedical Research, 250 Massachusetts Avenue, Cambridge, MA 02139. E-mail: darrin.stuart@novartis.com; and Mariela Jaskelioff, mariela.jaskelioff@novartis.com

doi: 10.1158/1541-7786.MCR-18-0327

wild-type melanoma cell lines, suggesting that cellular context is a critical factor.

Materials and Methods

Cell culture, vectors, viral production, and infection

Human cancer cell lines originated from the Cancer Cell Line Encyclopedia, authenticated by single-nucleotide polymorphism analysis and tested for *Mycoplasma* infection (19). All cell lines in the experiments were used within 4 weeks after thawing. WM793, UACC62, GR-M, MeWo, and Hs944.T were cultured in RPMI medium (Thermo Fisher Scientific); A-375 cells were grown in DMEM (Thermo Fisher Scientific); HMCB cells were grown in minimum essential medium (Thermo Fisher Scientific). All culture media were supplemented with 10% FBS (Thermo Fisher Scientific).

The cDNA for *MAPK1* (NM_002745) or *MAPK3* (NM_002746) in pENTR221 was cloned into pXP1509A (Supplementary Fig. S1A) using Gateway cloning (Thermo Fisher Scientific). The V600E mutation (t1799a) was introduced into *BRAF* (NM_004333) in pENTR221 by site-directed mutagenesis (QuikChange II, Agilent), and cloned into pXP1509A or pXP1512 (Supplementary Fig. S1A) using Gateway cloning (Thermo Fisher Scientific). The cDNA for NRAS Q61K (c181a) and MEK1 C121S (t361a) in pENTR221 (kindly provided by Kelli-Ann Monaco, Novartis Institutes for BioMedical Research) were cloned into pXP1509A (Supplementary Fig. S1A) using Gateway cloning (Thermo Fisher Scientific). The shRNA construct targeting *PSMA3* was cloned into the pLKO-Tet-On inducible vector system as described in ref. 20, and the following oligonucleotide sequence was used: CAAGCTGCAAAGACGGAAATA. The pMCSV_PGK-Luc vector was used for luciferase expression (kindly provided by Fangxian Sun, Genomics Institute of the Novartis Research Foundation). Viral constructs were packaged as described in ref. 20. Stable lines were selected and maintained in 800 μg/mL of G418 (Corning), 5 μg/mL blasticidin (Thermo Fisher Scientific), or 1 μg/mL puromycin (Corning). Doxycycline from Sigma-Aldrich was used for induction.

Cell viability and proliferation analysis

For short-term cell viability assays, 2,000 cells per well were seeded in triplicate in 96-well plates one day before compound addition and incubated for 3 days with various concentrations of compounds. Cell viability was determined by Cell Titer-Glo Luminescence Assay (Promega) as per the manufacturer's protocol. Luminescence signal was measured with an EnVision plate reader (PerkinElmer). The values were normalized to the signal from DMSO-treated cells (100% growth), cells on day 0 at the time of compound addition (0% growth), and cells completely killed with 10 μmol/L of MG132 (−100% growth). For the viability measurement of luciferase cells, Bright-Glo Luciferase Assay System (Promega) was used as per the manufacturer's protocol to measure the constitutive luciferase signal as a proxy for cell viability. The signal was measured and normalized as described above.

Proliferation was also measured using live-cell time-lapse imaging. Cells were seeded from 2,000 to 10,000 cells per well in triplicate in 96-well plates, and treated with or without 100 ng/mL doxycycline. Phase-contrast images were acquired at regular intervals using an IncuCyte ZOOM system (Essen BioScience) and confluence of the cultures was determined using IncuCyte software (Essen BioScience) over the time course as indicated. All experiments were independently performed at least two times; representative results are shown.

Western blot analysis

Whole-cell lysates were collected by directly lysing cells in plates with RIPA buffer (Thermo Fisher Scientific) plus protease inhibitor cocktail (Roche) and phosphatase inhibitor cocktail (Sigma). Protein concentrations were determined using a protein assay kit (Bio-Rad), and 15 μg of protein was loaded per lane. Antibodies against FRA1, pFRA1 (S265), ERK1/2, pERK1/2 (T202/Y204), RSK1/2/3, pRSK1 (T359), pRSK3 (T356/S360), DUSP4, PARP, LC3, pMEK1/2 (S217/S222), FOSB, p38, p-p38 (T180/Y182), CHOP, Ero1-Lα, p21, and H3 were from Cell Signaling Technology. Antibodies against DUSP6 and γH2A.X are from Abcam, MEK1 was from BD Biosciences, and pan-RAS was from Millipore. Chemiluminescent signal was detected using SuperSignal West Femto or Pico Maximum Sensitivity Substrate (Pierce), and visualized using Bio-Rad ChemiDoc Imaging System.

Intracellular immunofluorescence

Cells were harvested, pelleted, and washed in PBS, then fixed for 15 minutes in ice-cold 1% formaldehyde (methanol free, Pierce). After fixation, cells were washed in PBS and incubated in ice-cold methanol for 30 minutes. Cells were pelleted and washed in 1% BSA (fraction V, Rockland Immunochemicals) in PBS, then blocked 45 minutes at room temperature in 0.2% Triton X-100 + 3% normal goat serum (Cell Signaling Technology) in PBS. Cells were subsequently incubated for 2 hours in primary antibodies or isotype controls diluted in 0.1% Triton X-100 + 3% goat serum. Antibodies used were 2 μg/mL mouse anti-ERK1/2 (clone L34F12, Cell Signaling Technology) and 2 μg/mL mouse IgG1 (clone G3A1, Cell Signaling Technology). Next, the cells were washed as above, and incubated for 1 hour in 2 μg/mL anti-mouse Alexa 488–conjugated secondary antibody (Thermo Fisher Scientific). Finally, cells were washed as above, resuspended in 0.1% BSA in PBS, and analyzed using BD FACSCanto (BD Pharmingen). FACS results were analyzed using FlowJo v10 (FlowJo, LLC).

Cell-cycle and apoptosis analysis

For cell-cycle analysis, cells were plated in 6-well plates and analyzed after the indicated time of doxycycline induction. The supernatant was collected and combined with trypsinized cells, washed with 1× PBS, and fixed with 70% ethanol. Samples were stained with 10 μg/mL propidium iodide containing 0.25 mg/mL RNaseA at 37°C for 30 minutes. A total of 1×10^5 cells were measured with BD FACSCanto (BD Pharmingen) and analyzed with FlowJo (FlowJo, LLC). Watson (Pragmatic) model was used for the cell-cycle peak modeling.

Caspase activity was measured at the indicated times posttreatment using Caspase-Glo 3/7 assay (Promega) as per the manufacturer's protocol. Luminescence signal was measured with EnVision plate reader (PerkinElmer), and normalized to the control wells. TRAIL was purchased from PeproTech and zVAD-fmk from R&D Systems. All experiments were independently performed at least twice; representative results are shown.

Senescence was measured using Senescence β-Galactosidase Staining Kit (Cell Signaling Technology) according to manufacturer's protocol. Mitochondrial outer membrane polarization (MOMP) was measured using TMRE-Mitochondrial Membrane

Potential Assay Kit (Abcam) according to the manufacturer's protocol.

Pooled shRNA screen

The shRNA libraries and protocol used for pooled shRNA screens were described in ref. 21. Three shRNA libraries were screened as independent pools in A-375 ERK2 clone 10 cells. Briefly, 120 million cells were seeded the day before infection to achieve 1000X library representation. Twenty-four hours later, cells were infected with the lentiviral shRNA library at a MOI of 0.5, and selected with 1.5 μg/mL puromycin (Corning). After 7 days, infected cells were split into two pools, and treated with or without 100 ng/mL of doxycycline. Cells were cultured for an additional 11 days, splitting the cells as necessary and passaging 70 million cells each time. Cells were then harvested for gDNA extraction, and next-generation sequencing libraries were generated and sequenced.

Fold change (FC) of shRNA barcode representation was calculated between doxycycline-induced samples and control untreated samples, and further $\log_2$-transformed ($\log_2$_FC). $\log_2$_FC values were normalized to the activity distribution for each pool by calculating the robust *z*-score: $\log_2$_FC of shRNAx –median_$\log_2$_FC_all_shRNAs)/MAD_$\log_2$_FC_all_shRNAs), where MAD is the median absolute deviation. Upon comparing the three pools activity distributions, quantile normalization was applied prior to combining the results. Gene-level activity was determined by calculating two statistics. First, the RSA model was used to test whether the 20 shRNAs per gene showed consistent enrichment in the doxycycline-induced over untreated conditions (RSA Up test), producing a *P* value indicating the significance. Second, the robust *z*-score quartile Q1 or Q3 was determined per gene, representing the activity (rz-score) of the 25 and 75 percentile shRNA out of 20 tested for the gene, respectively (approximately activity of the 5th and 15th shRNA, respectively). The gene-level activity was shown (Fig. 4A) as $\log_{10}$ *P* value of RSA Up (logP_RSA_Up) as a function of the genes robust *z*-score Q3 (rz-score_Q3). For candidate gene hit selection, a threshold of $\log_{10}$ RSA $P < -5$ was chosen, as analysis of randomized datasets resulted in values above this threshold, along with an rz_score_Q3 > 3. The two thresholds are marked as dotted lines in the figure.

RNA-seq

Total RNA was isolated using the RNeasy Plus Mini Kit (QIAGEN) and quantified using RNA 6000 Nano Kit (Agilent Technologies) on Agilent 2100 BioAnalyzer. Two-hundred nanograms of high purity RNA (RNA Integrity Number 7.0 or greater) was used as input to the TruSeq Stranded mRNA Library Prep Kit, High Throughput (Illumina), and the sample libraries were generated per manufacturer's specifications on Hamilton STAR robotics platform. PCR-amplified RNA-Seq library products were then quantified with Fragment Analyzer Standard Sensitivity NGS Fragment Analysis Kit (Advanced Analytical Technologies). Samples were diluted to 10 nmol/L in Elution Buffer (QIAGEN), denatured, and loaded at a range of 2.5 to 4.0 pmol/L on an Illumina cBOT using HiSeq 4000 PE Cluster Kit (Illumina). RNA-Seq libraries were sequenced on a HiSeq 4000 at 75 base pair paired-end with 8 base pair dual indexes using HiSeq 4000 SBS Kit, 150 cycles (Illumina). Sequence intensity files were generated on instrument using Illumina Real Time Analysis software. Resulting intensity files were demultiplexed with the bcl2fastq2.

Transcript and gene expression analysis was performed using PISCES. Mutation discovery was performed as described in ref. 22. Briefly, FASTQ files were preprocessed for base quality and to remove adaptor sequences. They were then aligned with bowtie2 and a modified version of tophat1.3 against a custom genome or transcriptome FASTA file. Mutations were called using GATK best practices. FPKM values were generated using cufflinks version 2.0.2 against known transcripts from UCSC Known Genes (http://genome.ucsc.edu). RNA-seq data are available on the NCBI Sequence Read Archive, accession number SRP153919.

For Gene set enrichment analysis (GSEA), RNA-seq data were preranked with a score calculated by the product of $\log_2$ fold change and negative log *P* value. The analysis was conducted with GSEAPreranked tool using 1,000 permutations (23, 24).

Protein array

Quantitative proteomics array was performed by RayBiotech using Human Kiloplex Quantitative Proteomics Array (catalog no. QAH-CAA-X00-1) to measure concentrations of 1,000 proteins in conditioned media. Background levels in blank media control were subtracted from samples to calculate protein concentrations.

Database for Annotation, Visualization and Integrated Discovery (DAVID) was used to test for pathway enrichment in differentially secreted proteins (25, 26). *P* values of enriched functional annotations were adjusted using the Benjamini–Hochberg option.

Xenograft studies

Mice were maintained and handled in accordance with the Novartis Institutes for BioMedical Research (NIBR) Animal Care and Use Committee protocols and regulations. Female athymic nude mice were subcutaneously inoculated with 5 million A-375 cells overexpressing empty vector or ERK2 in 50% Matrigel + 50% PBS. Once average tumor volume reached 200 mm^3 in size, mice implanted with each cell line were randomized into doxycycline and control groups. Doxycycline was administered via diet supplementation (400 PPM; Pharmaserv). Tumor volume was measured twice weekly using calipers and calculated as (length × width × width)/2. For biomarker analysis, tumors were excised and snap frozen in liquid nitrogen. Whole-cell lysates were prepared by adding RIPA lysis buffer (Thermo Fisher Scientific) to tumor fragments and mechanically homogenizing with beads using TissueLyser (QIAGEN).

Histologic analysis and IHC

A-375 ERK2 clones 7 and 10 xenograft tumors were harvested at multiple time-points after treatment with doxycycline, formalin-fixed for 24 hours, processed, and paraffin embedded. Four-micron–thick histologic sections were stained with hematoxylin and eosin and analyzed by a pathologist. Percent of tumor cells, necrosis, and fibrosis out of total tumor area was manually quantified.

Results

Hyperactivation of MAPK signaling by ERK overexpression is cytotoxic in BRAF-mutant melanoma

To investigate the cellular response to MAPK hyperactivation, we sought to generate genetic models that would induce high levels of MAPK pathway signaling. We inducibly expressed

mutant alleles that occur in MAPK inhibitor–resistant melanoma ($NRAS^{Q61K}$, $BRAF^{V600E}$, $MEK1^{C121S}$; refs. 7, 8, 10, 14), as well as *MAPK1* (ERK2) or *MAPK3* (ERK1). Lentiviral constructs containing each gene expressed from a doxycycline-inducible promoter were stably transduced into A-375 cells, a $BRAF^{V600E}$ melanoma cell line. Induction of ERK1 or ERK2 overexpression resulted in a significant decrease in cell proliferation, whereas overexpression of $NRAS^{Q61K}$, $BRAF^{V600E}$, or $MEK1^{C121S}$ had minor effects, if any (Fig. 1A). To assess the effects of protein overexpression on MAPK signaling, lysates of the various cell lines were compared in the presence or absence of doxycycline. While ERK1 or ERK2 overexpression resulted in elevated levels of phosphorylated ERK1/2 substrates such as FRA, FOSB, and increased levels of DUSPs, overexpression of $NRAS^{Q61K}$, $BRAF^{V600E}$, or $MEK1^{C121S}$ had much milder effects, consistent with the minimal effects on proliferation (Fig. 1B and E). These results support the notion that levels of activated ERK are very tightly controlled and any perturbations will lead to significant growth effects. Given the strong effect of ERK2 overexpression on cell proliferation and MAPK signaling, we focused on this genetic model for further characterization.

Although ERK2 overexpression had a drastic effect on cell growth, it was unclear whether the entire cell population was growing more slowly, or if there was heterogeneity within the culture driven by different levels of ERK2 expression. Measurement of total protein levels of ERK1/2 by intracellular immunofluorescence revealed that indeed the cell population exhibited a wide range of ERK1/2 levels (Fig. 1C). We hypothesized that cells expressing lower levels of ERK2, comparable with that of parental cells, would be able to proliferate unperturbed, while those with the highest levels of ERK2 would suffer a fitness deficit. To test this hypothesis, subclones expressing various protein levels of ERK2 were isolated from the cell population. We successfully isolated three subclones that exhibited high levels of ERK1/2 protein in a range that largely did not overlap with that of the parental cells, and one subclone that expressed intermediate protein levels of ERK1/2 (Fig. 1D and E). We determined the growth rate of these clones after doxycycline exposure, and found that clones with high levels of ERK2 (clones 3, 7, and 10) did not proliferate appreciably over the course of the assay, whereas the intermediate clone (clone 12) was able to grow, but at a slower rate than parental or control cells not treated with doxycycline (Fig. 1F). Furthermore, consistent with our hypothesis that high ERK2 levels are not tolerated, long-term doxycycline treatment in the intermediate clone selected for cells with ERK1/2 levels that were similar to parental cells (Fig. 1G). In addition to A-375, we overexpressed ERK2 in two more $BRAF^{V600E}$ melanoma cell lines, WM793 and UACC62, and found they also exhibited proliferation defects upon ERK2 overexpression (Supplementary Fig. S1B and S1C). Taken together, our data showed that abnormally high levels of MAPK signaling were detrimental to the fitness of BRAF-mutant melanoma, and this effect seemed to be dose-dependent.

To test whether the effects of ERK2 overexpression were specific to its function in MAPK signaling, induction with doxycycline was combined with BRAF, MEK, or ERK inhibitors. In the absence of doxycycline, proliferation of A-375 ERK2 cells was inhibited by all three compounds in a dose-dependent manner, as expected for BRAF-mutant melanoma, which is dependent upon BRAF activity (Fig. 2A). Notably, induction of ERK2 overexpression alone had a cytotoxic effect (negative growth compared with day 0), whereas BRAF, MEK, or ERK inhibitors resulted in cell stasis. Combining MAPK inhibitors with doxycycline resulted in a bell-shaped response curve, indicating that effects of ERK2 overexpression were ameliorated by directly inhibiting the kinase activity of ERK (ulixertinib), or by blocking upstream signaling in the MAPK pathway (BRAF inhibitor, encorafenib; MEK inhibitor, trametinib), thereby decreasing the signaling output. Western blot analysis of MAPK pathway components and downstream targets supported this interpretation, as increased phosphorylation of ERK substrates induced by doxycycline was reversed by treatment with ERK inhibitor (Fig. 2B). These data indicated that the detrimental effects of ERK2 overexpression were attributable to hyperactivation of the MAPK signaling pathway, and not to nonspecific effects of excessive protein abundance.

To better understand the cellular response to MAPK hyperactivation, we profiled gene expression changes induced by ERK2 overexpression. mRNA was collected and sequenced from three A-375 clones containing the inducible ERK2 construct, treated for 6 or 20 hours with DMSO, doxycycline, or the ERK inhibitor ulixertinib. Genes that were significantly differentially expressed at 6 hours ($\log_2 FC < -1$ or > 1; $P < 1 \times 10^{-4}$) showed a strikingly inverse profile in the doxycycline condition compared with treatment with ERK inhibitor (Fig. 2C). This provided further evidence for the specific effects of ERK2 overexpression on the MAPK pathway.

GSEA of genes upregulated upon doxycycline exposure revealed a positive association with the KRAS signaling gene set (FDR q-value $< 1 \times 10^{-5}$), consistent with activation of MAPK signaling (Supplementary Table S1). Furthermore, genes with transcription factor motifs known to be regulated by ERK1/2, including AP-1, ETS, ELK-1, and EGR, were significantly enriched (Supplementary Table S2; ref. 27). Interestingly, the apoptosis and unfolded protein response gene sets were significantly associated with genes upregulated upon ERK2 overexpression (Supplementary Table S1), suggesting a role for apoptosis and ER stress responses in mediating cell death.

Hyperactivation of the MAPK pathway leads to induction of stress responses and apoptotic signaling

To investigate the cause of decreased cell viability upon ERK2 overexpression, A-375 cells were collected for cell-cycle analysis at various time points after doxycycline induction. The most substantial change observed was a dramatic, time-dependent increase in the sub-G_1 population after doxycycline treatment (Fig. 3A). Aside from a minor increase in the fraction of cells in the G_2–M phase, there was no significant change in any other stage of the cell cycle. This suggested that ERK2 overexpression predominantly resulted in cell death rather than cell-cycle arrest. Furthermore, the lack of accumulation of cells in any one stage of the cell cycle indicated that the activity of the downstream effector(s) responsible for this phenotype was not restricted to a particular cell-cycle stage. An examination of the morphologic changes induced by ERK2 overexpression revealed that cells were rounding up and detaching, consistent with cell death (Fig. 3B). Staining for senescence-associated β-galactosidase activity revealed no significant cell senescence, further supporting cell death as the main outcome of MAPK hyperactivation (Supplementary Fig. S2A).

Apoptosis is a well-studied process for programmed cell death, and is characterized biochemically by activation of caspases (28). To test whether apoptotic signaling was induced upon ERK2 overexpression, we measured the activity of caspase-3/7, the main effector caspases. Consistent with the observed cell death

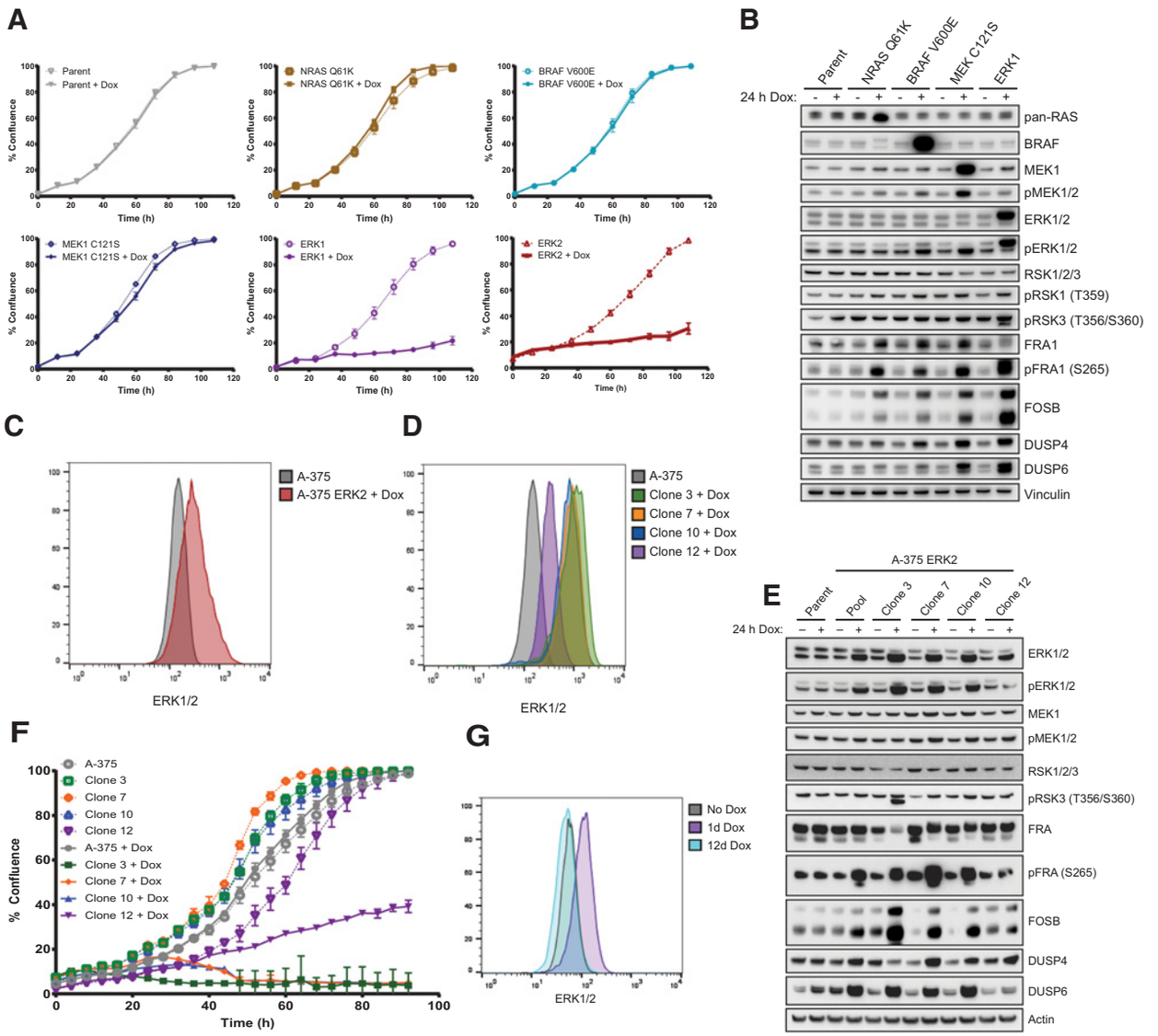

Figure 1.

Overexpression of ERK in A-375 led to loss of cell viability. **A,** Induction of ERK1 or ERK2 overexpression in A-375 cells dramatically decreased cell proliferation. Lentiviral infection was used to introduce $NRAS^{Q61K}$, $BRAF^{V600E}$, $MEK1^{C121S}$, ERK1, or ERK2 under control of a doxycycline-inducible promoter into A-375. Phase-contrast images were taken at the indicated time points following treatment ± 100 ng/mL doxycycline, and the percent confluence was determined. Error bars, SD of the mean of triplicate wells. **B,** Overexpression of ERK1 led to the most increased MAPK signaling. The indicated cell lines were treated ± 100 ng/mL doxycycline for 24 hours. Immunoblot analysis of total cell lysates was performed. **C,** The engineered A-375 cells expressed a wide range of ERK1/2 levels upon doxycycline treatment. The indicated cell populations were treated ± 100 ng/mL doxycycline for 24 hours and collected for intracellular immunofluorescence. Results from a representative experiment are shown. **D,** Subclones of A-375 stably expressing the inducible ERK2 construct were selected for different levels of ERK2 overexpression. ERK1/2 levels were measured as in **C**. **E,** Overexpression of ERK2 caused an increase in phosphorylation of ERK1/2 substrates. The indicated parent population, pool, or subclones of A-375 ERK2 cells were treated ± 100 ng/mL doxycycline for 24 hours. Immunoblot analysis of total cell lysates was performed. **F,** A-375 cells' sensitivity to ERK2 overexpression was proportional to the level of overexpression. Proliferation of subclones of A-375 ERK2 was measured as in **A**. **G,** Cells that survived doxycycline treatment had lower levels of ERK1/2. A-375 ERK2 clone 12 was treated ± 100 ng/mL doxycycline for 1 or 12 days, and ERK1/2 levels were measured as in **C**.

phenotype and the RNA-seq data, caspase-3/7 activity was increased more than 7-fold after 64 hours in doxycycline (Fig. 3C). MOMP, which often accompanies apoptosis and causes release of prodeath factors from the inner membrane space (IMS) into the cytoplasm (28), was also observed over time as cell viability decreased (Supplementary Fig. S2B).

To test the hypothesis that apoptosis was the primary mechanism for cell death when MAPK signaling exceeded physiologic levels, we attempted to block the effects of ERK2 overexpression by treatment with the pan-caspase inhibitor, zVAD-fmk. Although treatment with zVAD was able to rescue the cell death induced by TNF-related apoptosis-inducing ligand (TRAIL), it had no effect

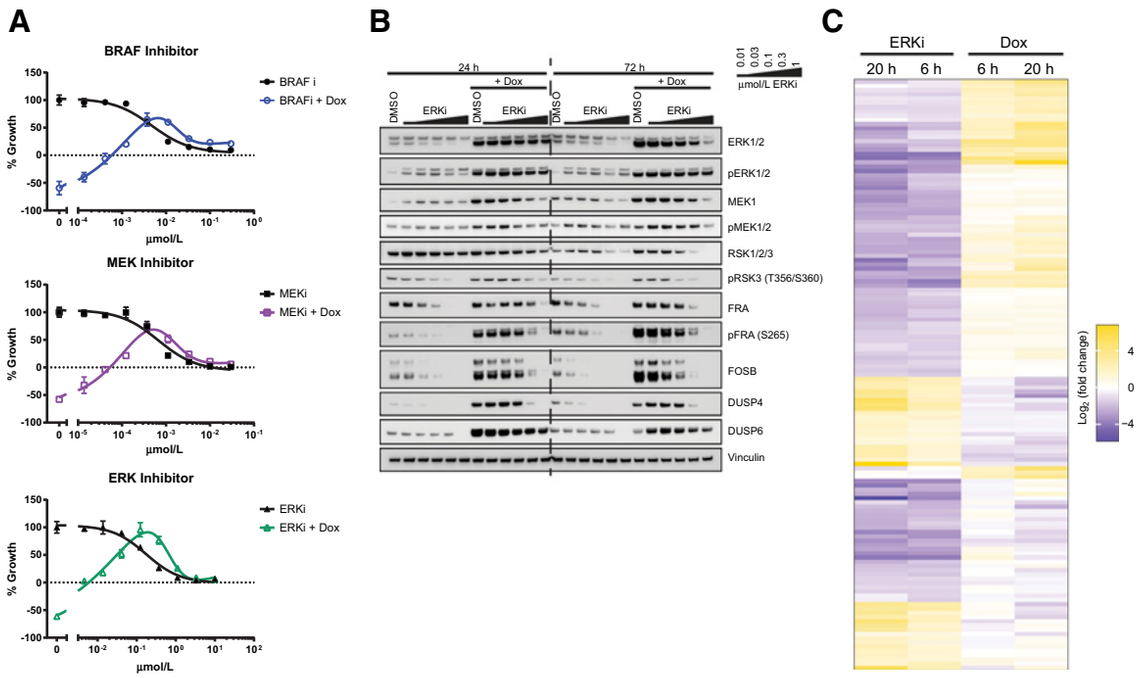

Figure 2.

The effects of ERK2 overexpression were reversed by MAPK inhibition. **A,** Treatment with MAPK inhibitors ameliorated the proliferation defect caused by overexpression of ERK2. A-375 ERK2 clone 10 was treated with the indicated concentrations of BRAF inhibitor (encorafenib), MEK inhibitor (trametinib), or ERK inhibitor (ulixertinib), and ± 100 ng/mL doxycycline. Cell viability was measured after 3 days using CellTiter-Glo, and normalized to the DMSO control and day 0 values. Error bars, SD of the mean of triplicate wells. **B,** Rescue of cell proliferation was accompanied by a corresponding reduction in MAPK pathway signaling. A-375 ERK2 clone 10 was treated ± 100 ng/mL doxycycline and the indicated concentrations of ERK inhibitor (ulixertinib) for 24 hours. Immunoblot analysis of total cell lysates was performed. **C,** Transcriptome profile of A-375–overexpressing ERK2 confirmed hyperactivation of the MAPK pathway. Heatmap shows the $\log_2$ of fold change values for genes that were significantly differentially expressed at 6 hours posttreatment ($\log_2$ FC > 1 or < −1; $P < 0.0001$). Values shown are the average of A-375 ERK2 clone 3, clone 7, and clone 10. Cells were treated with 100 ng/mL doxycycline or 1 µmol/L of ERK inhibitor (ulixertinib) for 6 or 20 hours, and total RNA was collected and sequenced.

on the loss of cell viability caused by ERK2 overexpression (Fig. 3D). Taken together, these data suggested that although caspases were activated in A-375 cells upon MAPK hyperactivation, they were not required for cell death.

With the purpose of further dissecting the events triggered by MAPK hyperactivation, we evaluated other cellular stress response pathways at various time points after ERK2 overexpression. A substantial increase in ERK2 protein levels was observed by 16 hours of doxycycline treatment, accompanied by a corresponding increase in MAPK signaling, as indicated by levels of pERK1/2 and the ERK1/2 targets FOSB and DUSP6 (Fig. 3E). Cleaved PARP was detected at 48 hours, consistent with the increase of caspase activity as measured previously. The cell-cycle inhibitor p21 also exhibited elevated levels at later time points. We also evaluated LC3-I levels and observed very little conversion to LC3-II, the form conjugated to phosphatidylethanolamine (PE) and indicative of autophagy (29). DNA damage response signaling was observed at late time points after 64 hours of doxycycline treatment, indicated by the increase in phosphorylation of H2A.X at Ser139 (γH2A.X; ref. 30). There was evidence of ER stress (unfolded protein response), as CHOP levels were substantially increased at 40 hours, along with a concomitant increase in the levels of its downstream target, ERO1-Lα (31). The p38 kinase, which is known to be activated upon cellular stress (32), was increasingly phosphorylated starting at 24 hours of doxycycline treatment. Similar stress responses were observed in the other A-375 ERK2 subclones, albeit at slightly different time points (Supplementary Fig. S2C). In summary, a widespread state of cellular stress was induced by MAPK hyperactivation with pleiotropic effects on multiple stress pathways.

Inhibition of cell proliferation induced by ERK2 overexpression is partially mediated by secreted factors

To investigate the effectors mediating the cell proliferation defect resulting from ERK2 overexpression, we conducted a large-scale pooled shRNA screen using a library targeting approximately 7,800 genes with an average of 20 shRNAs per gene (21). A-375 ERK2 cells infected with lentiviral particles containing the shRNA library were cultured for 7 days in the presence of the selection agent. The cells were then split into two arms, treated with or without doxycycline to induce ERK2 overexpression, and the pools of cells were cultured for an additional 11 days before gDNA was collected for next-generation sequencing. Overexpression of ERK2 led to massive cell death as expected, with a small number of live cells remaining, presumably expressing shRNAs that enabled them to survive. The top shRNAs that ameliorated the effect of ERK2 overexpression were those targeting *BRAF* and *MAP2K1* (MEK1; Fig. 4A; Supplementary Table S3). This result further confirmed that the cytotoxic effect of ERK2 overexpression was due to MAPK hyperactivation, as knockdown of upstream

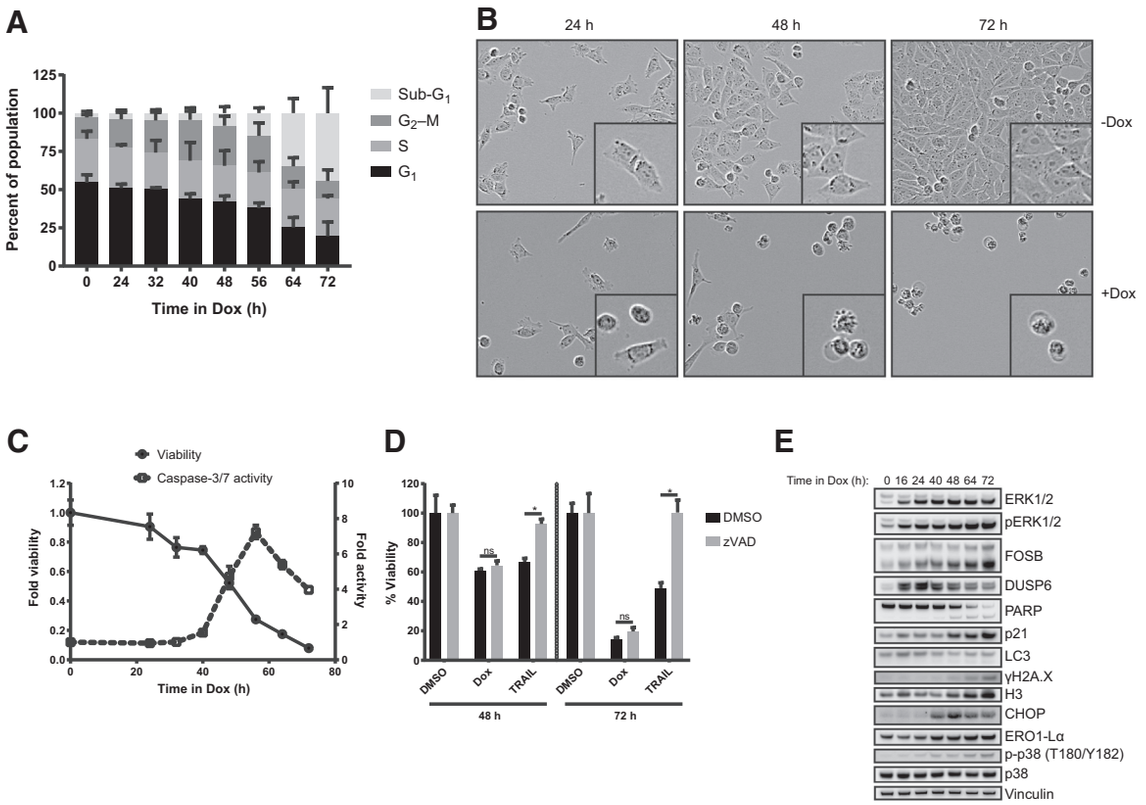

Figure 3.

ERK2 overexpression in A-375 cells resulted in activation of stress response and apoptotic pathways. **A,** ERK2 overexpression resulted in accumulation of cells in the sub-G_1 fraction. A-375 ERK2 clone 10 was treated with 100 ng/mL doxycycline for the indicated time points. Attached and floating cells were fixed, stained with propidium iodide, and analyzed by flow cytometry. Error bars, SD of the mean of three independent experiments. **B,** Cells showed morphologic changes after overexpression of ERK2. Phase-contrast images were taken of A-375 ERK2 clone 10 cells at the indicated time points following treatment ± 100 ng/mL doxycycline. Representative images are shown. **C,** Caspase-3/7 activity increased after overexpression of ERK2. A-375 ERK2 clone 10 was treated with 100 ng/mL doxycycline for the indicated time points. Viability was determined using CellTiter-Glo, and caspase-3/7 activity was measured using the Caspase-Glo 3/7 Assay, and values were normalized to untreated cells. Error bars, SD of the mean of triplicate wells. **D,** Inhibition of caspase activity did not rescue the loss of cell proliferation induced by ERK2 overexpression. A-375 ERK2 clone 10 was treated with 100 ng/mL doxycycline, 50 ng/mL TRAIL, or 50 μmol/L zVAD in the indicated combinations for 48 or 72 hours. Viability was determined using CellTiter-Glo, and values were normalized to the DMSO control. Error bars, the SD of the mean of triplicate wells. Statistical testing was performed using Student *t* test with the Holm–Šídák method of multiple testing correction (ns, nonsignificant; *, $P < 0.001$). **E,** Multiple stress pathways were induced in response to ERK2 overexpression in A-375. A-375 ERK2 clone 10 was treated ± 100 ng/mL doxycycline for the indicated time points. Immunoblot analysis of total cell lysates was performed.

nodes of the pathway was able to counteract the effect. As expected, shRNAs targeting *MAPK1* (ERK2) itself also strongly rescued MAPK hyperactivation–induced cell death (not shown in Fig. 4A as the *P* value was lower than the lowest reportable; Supplementary Table S3). The lack of other shRNAs able to provide a growth benefit in the presence of MAPK hyperactivation suggested that there were multiple effectors downstream of ERK2 contributing to the cell death phenotype, or redundancy at specific pathway nodes, so that knockdown of any one single gene was not enough to escape this fate.

Another factor that complicates the interpretation of pooled shRNA screens is the contribution of secreted factors leading to paracrine signaling, which could mask the effect of individual shRNAs in neighboring cells. Indeed, GSEA revealed enrichment of the inflammatory response and secreted proteins gene sets in genes upregulated upon doxycycline induction (Supplementary Table S1), further suggesting a secretory component of the phenotype induced by ERK2 overexpression. To test this hypothesis, we collected conditioned media from A-375 ERK2 cells treated without or with doxycycline for 24 or 48 hours, and transferred them to parental A-375 cells. While the control (no doxycycline) conditioned media had a small effect on cell proliferation, presumably due to nutrient depletion, the conditioned media collected from cells overexpressing ERK2 resulted in markedly decreased growth of parental A-375 cells, with the maximal effect observed from conditioned media following 48 hours of doxycycline treatment (Fig. 4B). This reduction in cell proliferation, although significant, did not reach the same magnitude observed in the cells directly overexpressing ERK2, indicating that the secreted factor(s) is but a part of the complex cellular response that results in cell death. To validate these unexpected results using an orthogonal system, we cocultured A-375 cells engineered to constitutively express luciferase (A-375-Luc) with either parental A-375 cells, or A-375 ERK2, and treated with or without doxycycline. Luciferase signal intensity was determined after 72 hours as a readout of the A-375-Luc growth rate. Consistent with the

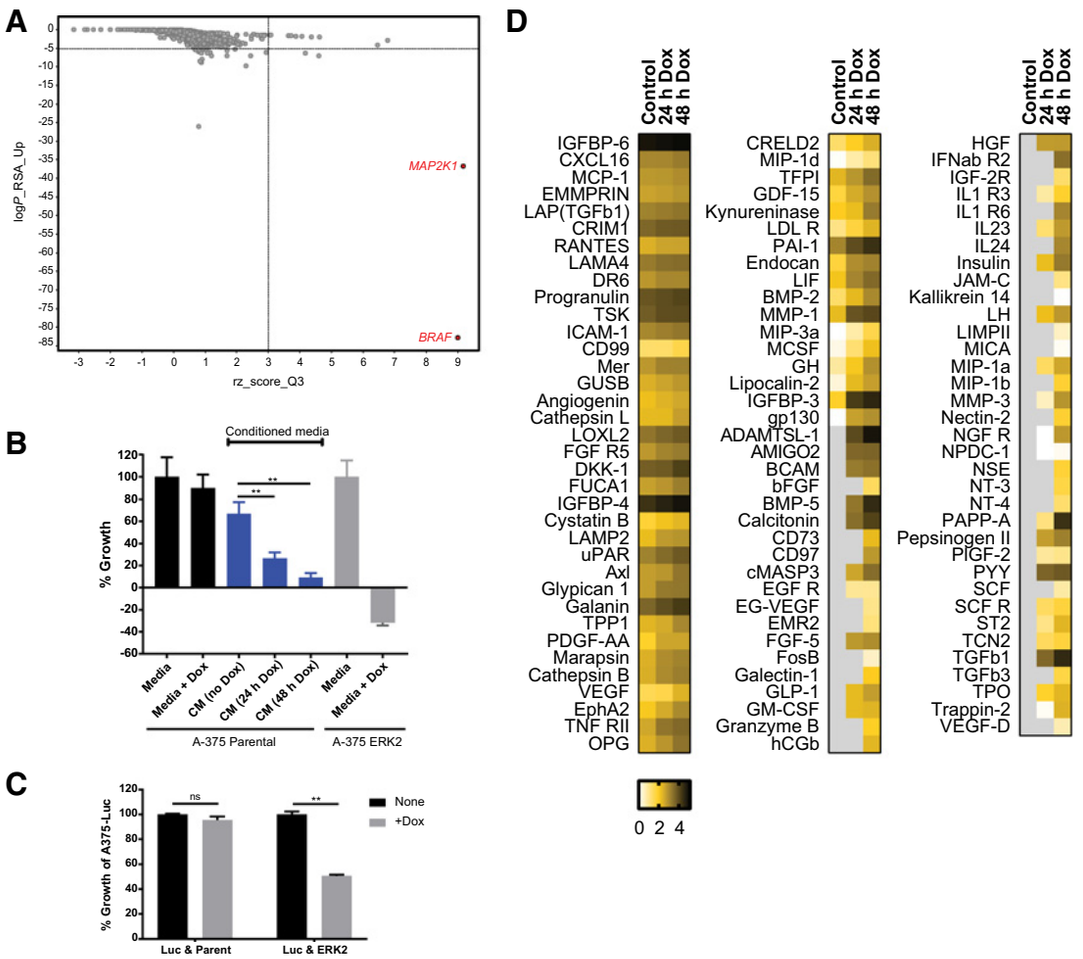

Figure 4.

Inhibition of cell proliferation induced by ERK2 overexpression was partially mediated by secreted factors. **A,** Knockdown of *BRAF* or *MAP2K1* rescued the growth defect of A-375 cells overexpressing ERK2. A-375 ERK2 clone 10 was infected with lentiviral particles containing a pooled shRNA library, and then treated ± 100 ng/mL doxycycline for 14 days. shRNA representation from both populations was determined by next-generation sequencing. The plot shows RSA *P* values and Q3-*z*-scores for all shRNAs at the gene level in doxycycline-treated versus control conditions. **B,** Reduced proliferation was observed in cells exposed to conditioned media (CM) from A-375 cells overexpressing ERK2. CM produced from A-375 ERK2 clone 10 treated ± 100 ng/mL doxycycline for the indicated time points were transferred to parental A-375 cells. Cell viability of the parental cells was measured after 3 days using CellTiter-Glo, and normalized to the media control and day 0 values. Error bars, SD of the mean of triplicate wells. Statistical testing was performed using one-way ANOVA (**, $P < 0.0001$). **C,** Cells cocultured with A-375–overexpressing ERK2 showed reduced proliferation. A-375-Luc was cocultured at a 1:1 ratio with either parental A-375 or A-375 ERK2 clone 10, and treated ± 100 ng/mL doxycycline for 3 days. Bright-Glo was used to measure the luciferase signal, and was normalized to the control condition for each cell mixture. Error bars, SD of the mean of triplicate wells. Statistical testing was performed using Student *t* test with the Holm–Šídák method of multiple testing correction (ns, nonsignificant; **, $P < 0.0001$). **D,** More than 100 soluble proteins were differentially secreted by A-375–overexpressing ERK2. CM from A-375 ERK2 clone 10 treated ± 100 ng/mL doxycycline for 24 or 48 hours were collected, and the concentrations of 1,000 proteins were measured using a quantitative proteomics array. The heatmap shows log of concentrations (log[pg/mL]) of the proteins that increased upon doxycycline treatment. Gray indicates the protein concentration was below background levels of the blank media control.

previous experiment, growth of A-375-Luc cells was reduced by coculture with A-375 cells only when ERK2 was overexpressed, but was unaffected by coculture with parental A-375 cells, or the control condition without doxycycline (Fig. 4C). Importantly, this paracrine effect was not generally observed in all dying cells, as conditioned media from A-375 cells expressing an shRNA targeting the essential gene *PSMA3* (A-375 shPSMA3) did not hinder cell proliferation, nor did coculture with A-375 shPSMA3 cells (Supplementary Fig. S3). Taken together, these results were consistent with a cell-extrinsic factor(s) mediating the antiproliferative effect of MAPK activity beyond a tolerated threshold.

To evaluate what proteins were differentially secreted upon ERK2 overexpression, we utilized a quantitative proteomics array to measure the concentrations of 1,000 target proteins in the conditioned media from A-375 ERK2 cells treated without or with doxycycline for 24 or 48 hours. A total of 107 proteins displayed time- and doxycycline-dependent accumulation in the conditioned media (Fig. 4D). Using DAVID to identify enriched

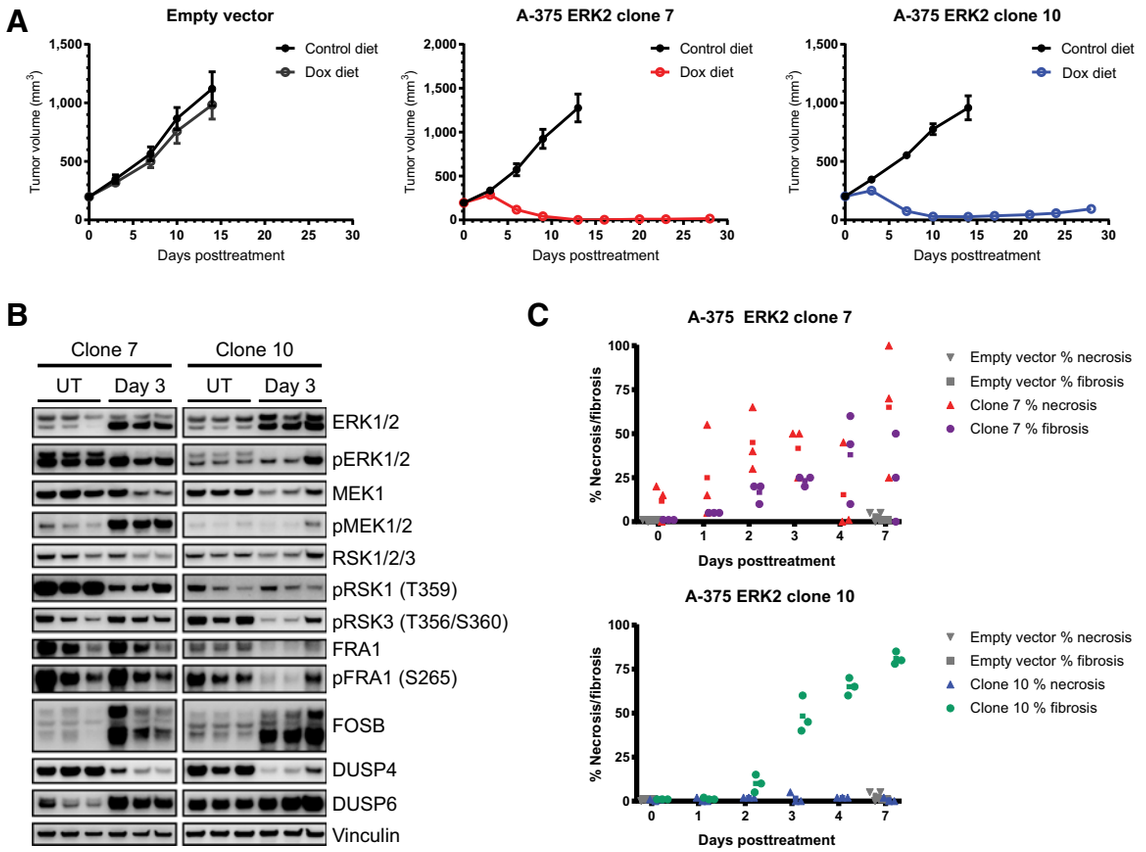

Figure 5.

Hyperactivation of MAPK pathway in a BRAF-mutant melanoma xenograft model led to complete tumor regression. **A,** Mice bearing xenografts of A-375–expressing empty vector, A-375 ERK2 clone 7, or A-375 ERK2 clone 10 were kept on a diet supplemented with or without doxycycline. Data are represented as mean tumor volume (mm^3) ± SEM. Each group included 8 animals. **B,** Overexpression of ERK2 led to increased MAPK signaling in the A-375 xenograft tumors. Immunoblot analysis of MAPK signaling markers was performed on tumor fragments from the untreated (UT) group or 3 days posttreatment using 3 animals per treatment group. **C,** Tumors induced to overexpress ERK2 showed increasing necrotic or fibrotic areas over time. Hematoxylin and eosin–stained histologic sections of the tumor fragments collected at the indicated time points were assessed for the fraction of the tumor area that exhibited necrosis or fibrosis.

pathways over the background of the proteins on the array revealed the KEGG pathway rheumatoid arthritis ($P_{adj} < 0.05$), suggesting that MAPK hyperactivation may be inducing pro-inflammatory factors. This includes members of the CC-chemokine class, MIP-1a, MIP-1b, MIP-1d, MIP-3a, RANTES, and MCP-1, the matrix metalloproteinases, and signaling factors such as TGFβ1, GM-CSF, and VEGF. Taken together, these results indicated that secreted factors contributed to the antiproliferative effects of MAPK hyperactivation in BRAF-mutant melanoma.

MAPK hyperactivation leads to tumor regression in an A-375 xenograft model

Because hyperactivation of the MAPK pathway led to dramatic cytotoxic effects *in vitro* and could represent a novel therapeutic approach, we sought to confirm the effects of ERK2 overexpression on tumor growth *in vivo*. Two subclones of A-375 that expressed high levels of ERK2, or A-375 cells harboring an empty expression vector, were implanted subcutaneously into nude mice. When the average tumor size reached 200 mm^3, mice were randomized to two groups that were fed diets supplemented with or without doxycycline. Robust tumor regression was observed in A-375 xenografts expressing high levels of ERK2, starting 3 days posttreatment, and achieving complete regression by 10 days (Fig. 5A). In contrast, A-375 tumors harboring the empty vector grew at the same rate regardless of doxycycline exposure (Fig. 5A). Western blots of protein lysates from tumor fragments confirmed the overexpression of ERK2 in the doxycycline-treated groups, with a corresponding increase in pERK1/2, and the ERK1/2-regulated proteins FOSB and DUSP6 (Fig. 5B). Hematoxylin and eosin staining of tumor fragments revealed a time-dependent increase in the fraction of necrotic or fibrotic cells in the subclones with overexpression of ERK2, but not in the empty vector control (Fig. 5C; Supplementary Fig. S4). Thus, MAPK hyperactivation induced robust cell death *in vivo* in a BRAF-mutant melanoma xenograft model, leading to complete tumor regression.

ERK2 overexpression is detrimental to RAS/RAF-mutant, but not RAS/RAF wild-type melanoma cell lines

We hypothesized that the dramatic effect of ERK2 overexpression on the proliferation of A-375 cells was dependent on the high basal levels of MAPK signaling conferred by constitutively active

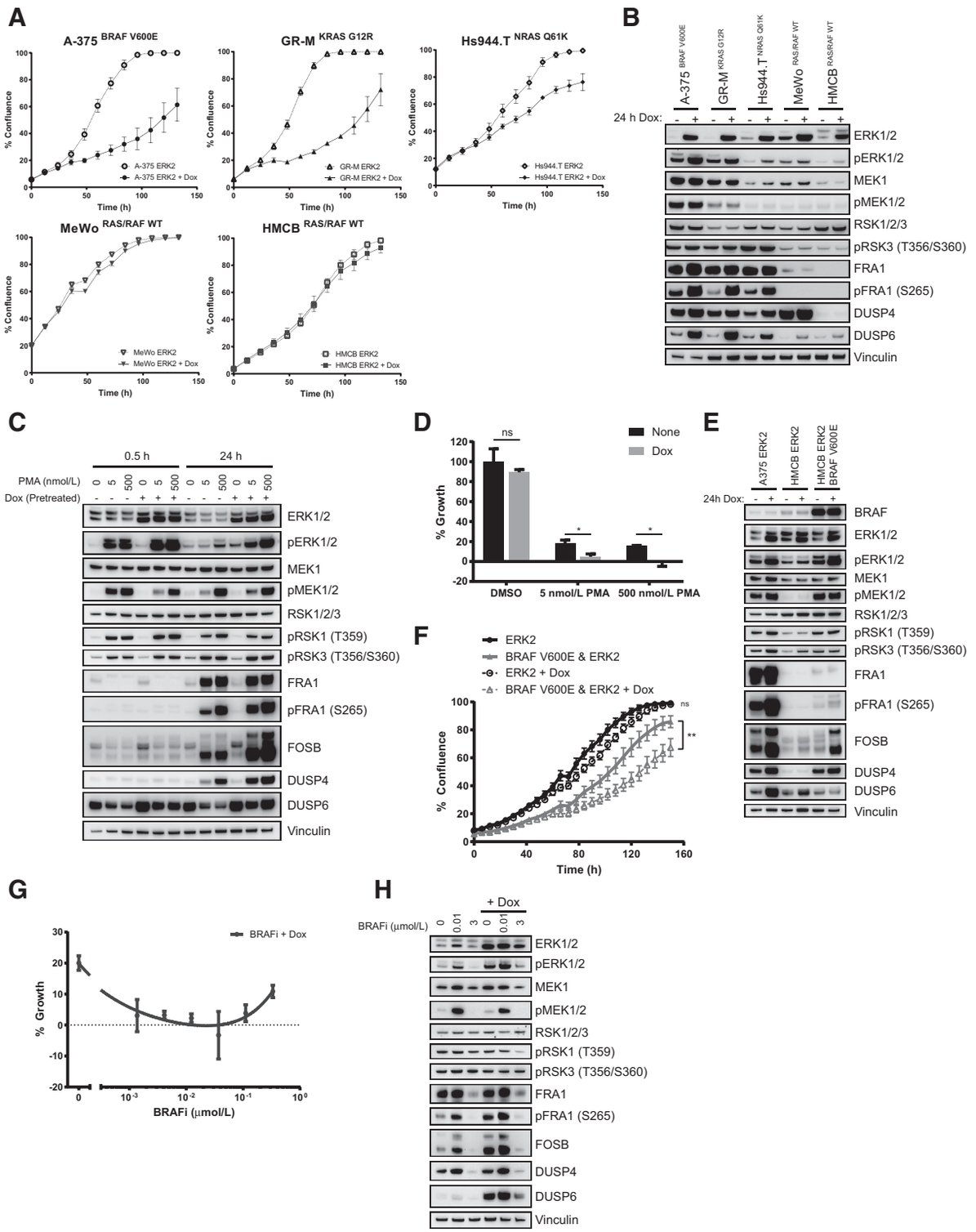

Figure 6.

ERK2 overexpression was detrimental to melanoma cell lines with RAS or RAF mutations, but not those wild-type for RAS and RAF. **A,** ERK2 was overexpressed in 5 melanoma cell lines with different RAS and RAF mutation statuses. Phase-contrast images were taken at the indicated time points following treatment ± 100 ng/mL doxycycline, and the percent confluence was determined. Error bars, SD of the mean of triplicate wells. **B,** ERK2 overexpression increased downstream pathway activity to different levels in each melanoma cell line. Each engineered cell line was treated ± 100 ng/mL doxycycline for 24 hours. Immunoblot analysis of total cell lysates was performed. (*Continued on the following page.*)

$BRAF^{V600E}$. To explore the importance of cellular context, we tested the effect of ERK2 overexpression on melanoma cell lines with different RAS/RAF mutations or with wild-type RAS and RAF. To this end, additional melanoma cell lines with different driver mutations were stably transduced with the lentivirus-inducible ERK2 construct, and their proliferation was tested in the presence of doxycycline. In addition to A-375, two other cell lines with MAPK mutations, GR-M ($KRAS^{G12R}$) and Hs944.T ($NRAS^{Q61K}$), exhibited decreased proliferation when treated with doxycycline, whereas in the two RAS/RAF wild-type cell lines (MeWo and HMCB), ERK2 overexpression resulted in minimal effect on cell growth (Fig. 6A). Western blot analysis of the panel of cell lines revealed that RAS/RAF wild-type cell lines had overall less MAPK signaling; in particular, there were lower levels of pMEK and very low levels of the ERK1/2 substrate FRA1 (Fig. 6B). Taken together, the data suggested that cell lines with constitutively activating RAS/RAF mutations, and thereby high levels of MAPK signaling, were more susceptible to a detrimental hyperactivation state induced by ERK2 overexpression. A nonexclusive alternative is that the RAS/RAF wild-type cell lines may be better able to adapt to the influx of additional ERK2 activity by more effectively modulating the pathway output through negative regulation.

Although total ERK2 was increased in the RAS/RAF wild-type cell lines upon doxycycline induction, pERK1/2 levels were not substantially changed, indicating that the surplus ERK2 proteins were not activated, and thus had no effect on downstream signaling output. To test whether the lack of effect of ERK2 overexpression in RAS/RAF wild-type cells was due to the inability to activate excess ERK2 molecules, we used two approaches to activate ERK2 in these cells. First, phorbol 12-myristate 13-acetate (PMA), a PKC activator, was used to induce MAPK signaling in the HMCB cell line (RAS/RAF wild-type). Treatment with PMA was able to robustly activate MAPK signaling, as measured by Western blotting of ERK1/2 substrates and ERK1/2-regulated proteins (Fig. 6C). Induction of pERK1/2 by PMA at 0.5 hours was suppressed by 24 hours, showing evidence of active negative pathway modulation in HMCB cells. Proliferation of HMCB ERK2 cells was reduced by treatment with PMA, and the effect was further enhanced when ERK2 overexpression was induced by doxycycline treatment (Fig. 6D). Notably, the cytotoxicity caused by MAPK hyperactivation in this RAS/RAF wild-type cell line was not as severe as in a BRAF-mutant cell line, highlighting the importance of cellular context.

In the second approach, constitutive expression of ectopic $BRAF^{V600E}$ was engineered into HMCB cells harboring the inducible ERK2 construct. Introduction of $BRAF^{V600E}$ significantly elevated MAPK signaling to levels comparable with A-375 ($BRAF^{V600E}$ melanoma), as assessed by Western blotting (Fig. 6E). Overexpression of ERK2 in HMCB cells expressing $BRAF^{V600E}$, but not parental cells, further increased MAPK signaling, and resulted in significantly reduced proliferation despite the differences in initial seeding density of the cell lines (Fig. 6E and F). Taken together, these data indicated that RAS/RAF wild-type melanoma cells were not susceptible to the toxic effects of ERK2 overexpression without additional perturbations to increase MAPK signaling, supporting the hypothesis that RAS/RAF wild-type melanoma cells have lower basal levels of MAPK signaling and more effective negative feedback regulation compared with RAS/RAF-mutant melanoma tumors.

Given the striking effects of MAPK hyperactivation on RAS/RAF-mutant tumors, we sought to explore potential approaches for therapeutic intervention leveraging this mechanism of action. MAPK pathway activation by a pharmacologic agent has been previously reported upon treatment of RAS-mutant tumors with first-generation BRAF inhibitors, which lead to paradoxical activation of MAPK signaling (33–36). We reasoned that this paradoxical activation could be combined with ERK2 overexpression to further increase MAPK output beyond a tolerated threshold. Consistent with this hypothesis, a low dose of BRAF inhibitor (encorafenib) resulted in paradoxical activation of MAPK signaling in GR-M ERK2 cells ($KRAS^{G12R}$), and cell viability was further reduced when combined with ERK2 overexpression (Fig. 6G and H). In contrast, a high dose of BRAF inhibitor, which suppressed MAPK signaling, partially rescued the impact of ERK2 overexpression (Fig. 6G and H; Supplementary Fig. S5).

Discussion

In this study, we generated and characterized an isogenic model of MAPK hyperactivation by overexpressing ERK2 in an inducible manner in a $BRAF^{V600E}$ melanoma cell line. Supraphysiologic levels of ERK2 were detrimental to proliferation of A-375 cells in a dose-dependent manner *in vitro*, and led to tumor regression in an *in vivo* xenograft model. The MAPK hyperactivation–induced cell death *in vitro* was fully rescued with MAPK inhibitors, indicating that ERK catalytic activity was required, in contrast to noncatalytic effects of ERK2 reported in other systems (37). Moreover, the transcriptional profile resulting from ERK2 overexpression showed a strikingly opposite pattern to that of the transcriptional profile produced by ERK inhibition, further supporting the

(*Continued.*) **C,** Treatment with PMA induced MAPK signaling, which was further increased upon overexpression of ERK2 in HMCB. HMCB ERK2 cells were pretreated ± 100 ng/mL doxycycline for 1 day, and then treated with the indicated concentrations of PMA for 0.5 or 24 hours. Immunoblot analysis of total cell lysates was performed. **D,** Stimulation of MAPK signaling with PMA sensitized HMCB to ERK2 overexpression. HMCB ERK2 cells were pretreated for 24 hours ± 100 ng/mL doxycycline, and then treated with the indicated concentrations of PMA. Cell viability was measured after 3 days using CellTiter-Glo, and normalized to the DMSO control and day 0 values. Error bars, SD of the mean of triplicate wells. Statistical testing was performed using Student *t* test with the Holm–Šídák method of multiple testing correction (ns, nonsignificant; *, $P < 0.05$). **E,** Constitutive expression of $BRAF^{V600E}$ in HMCB resulted in higher MAPK signaling, which was further increased by ERK2 overexpression. The indicated cell lines were treated ± 100 ng/mL doxycycline for 24 hours. Immunoblot analysis of total cell lysates was performed. **F,** Elevating levels of MAPK signaling by introduction of the $BRAF^{V600E}$ oncogene into HMCB resulted in sensitization to ERK2 overexpression. HMCB ERK2 cells with or without constitutive expression of $BRAF^{V600E}$ were treated ± 100 ng/mL doxycycline. Phase-contrast images were taken at the indicated time points, and the percent confluence was determined. Error bars, SD of the mean of triplicate wells. Statistical testing was performed using Student *t* test on the 150-hour time point (ns, nonsignificant; **, $P < 0.0001$). **G,** Paradoxical activation induced by low doses of BRAFi in GR-M augmented the growth suppression caused by ERK2 overexpression. GR-M ERK2 cells were treated with the indicated concentrations of BRAF inhibitor (encorafenib) and 100 ng/mL doxycycline. Cell viability was measured after 3 days using CellTiter-Glo, and normalized to the DMSO control and day 0 values. Error bars, SD of the mean of triplicate wells. **H,** MAPK signaling was activated or suppressed by BRAFi in GR-M, depending on the dose. GR-M ERK2 was treated ± 100 ng/mL doxycycline and the indicated concentrations of BRAF inhibitor (encorafenib) for 24 hours. Immunoblot analysis of total cell lysates was performed.

hypothesis that ERK2 overexpression leads to cell death through specific effectors downstream of the MAPK pathway. Although MAPK hyperactivation in A-375 cells resulted in increased caspase activity, it was not required for cell death. The exact mechanisms of cell death are still unknown, but the observations that MAPK hyperactivation led to activation of not only caspases, but also ER stress and DNA damage signaling pathways, lead us to speculate that ERK2 overexpression induces a plethora of cellular responses that overwhelm the cell and cause its demise.

To identify mediators of MAPK hyperactivation–induced cell death, we conducted a large-scale pooled shRNA screen. We found that only knockdown of upstream nodes of the MAPK pathway could rescue ERK2 overexpression–induced death, providing further evidence to support the hypothesis that MAPK hyperactivation leads to pleiotropic effects on downstream cellular pathways. In a recent report, knockout of *JUNB*, which is known to be regulated by ERK1/2, rescued cell death induced by MAPK inhibitor withdrawal in drug-resistant cells (17). *JUNB* shRNAs were not enriched in our screen, which may be due to differences in the screening format or changes that drug-resistant cells undergo compared with treatment-naïve cells. Another possible explanation for the lack of rescuers in the pooled shRNA screen stems from our discovery that secreted factors contributed to the antiproliferative effect of MAPK hyperactivation. This paracrine effect constitutes, to our knowledge, the first report of such a mechanism of action. Although we identified more than 100 proteins that were differentially secreted by ERK2-overexpressing cells, the mechanisms by which these secreted factors can inhibit cell proliferation are still unclear. Some signaling factors may have antiproliferative effects, such as TGFβ1 (38). Alternatively, growth factors may be activating additional signaling pathways and exacerbating the hyperoncogenic state. Further experiments are needed to elucidate the underlying molecular mechanisms.

We report here that ERK2 overexpression was detrimental to RAS/RAF–driven melanoma cell lines, but had negligible effects on RAS/RAF wild-type cell lines, likely due to lower baseline levels of MAPK signaling. In RAS/RAF-mutant tumors, much of the negative regulation of the upstream nodes of the pathway is ineffective (39, 40). Specifically in RAF-mutant tumors, MAPK signaling is kept in check by upregulation of negative regulators of ERK1/2, such as DUSPs (41). Our data suggest that ERK1/2 protein abundance might be a rate-limiting factor that regulates pathway output. Increasing concentrations of ERK2 protein through ectopic overexpression presumably shifts the equilibrium between active and inactive ERK1/2 molecules, resulting in increased signaling output. In contrast, RAS/RAF wild-type tumors control the amount of MAPK signaling via negative regulation, as indicated by lower baseline levels of pMEK1/2, and thus excess ERK2 molecules are not phosphorylated. Only when the baseline levels of MAPK signaling, and thus ERK2 phosphorylation, are elevated using chemical or genetic means, do cells become vulnerable to ERK2 overexpression and consequent MAPK hyperactivation.

There is mounting evidence that the levels of MAPK signaling must be finely tuned and cannot be tolerated at supraphysiologic levels. This balance can be upset by introducing gain-of-function perturbations at multiple nodes in the MAPK pathway, such as overexpressing ERK2 or mutant BRAF in RAS/RAF-mutant melanoma (this study; refs. 42, 43), or coexpression of oncogenic mutations of EGFR and KRAS in lung adenocarcinoma (44). MAPK hyperactivation can also be achieved by removing the inhibitory pressure of MAPK inhibitors in drug-resistant tumor cells that have upregulated MAPK signaling (15–18, 45). This so-called "Goldilocks principle" of just the right amount of signaling has also been observed in other signaling pathways. In anaplastic large-cell lymphoma (ALCL) driven by the NPM-ALK fusion kinase, tumor cells develop resistance to ALK inhibitor by upregulation of ALK kinase activity. Mirroring the situation for drug-resistant melanoma tumors, resistant ALCL tumor cells are similarly addicted to the ALK inhibitor, and exhibit increased ALK signaling and cell death or arrest (46). The well-studied phenomenon of oncogene-induced senescence also describes the effects of increased oncogenic signaling, but in the context of nontransformed cells with basal levels of signaling (47). In contrast, cell death induced by MAPK hyperactivation occurs when tumor cells with oncogenic levels of signaling increase the signaling even further to supraphysiologic levels. Thus, the cellular context and levels of signaling differentiate between these related but distinct phenomena.

Identification of the detrimental effects of hyperoncogenic signaling reveals a novel vulnerability of tumors that have become resistant to MAPK inhibitors. In tumors where the mechanism of resistance is reactivation of the pathway, a drug holiday may induce MAPK hyperactivation and tumor regression, an approach we and others have investigated (15–17). Further exploration of mechanisms and contexts of MAPK hyperactivation is needed, and could lead to new avenues of cancer therapies.

Disclosure of Potential Conflicts of Interest

F.D. Sigoillot has ownership interest (including stock, patents, etc.) in Novartis. J.A. Engelman is the head of oncology at Novartis Institute for Biomedical Research and has ownership interest (including stock, patents, etc.) in Novartis. M. Jaskelioff has ownership interest (including stock, patents, etc.) in Novartis. D.D. Stuart has ownership interest (including stock, patents, etc.) in Novartis. No potential conflicts of interest were disclosed.

Authors' Contributions

Conception and design: G.P. Leung, A.K. Freeman, M. Jaskelioff, D.D. Stuart
Development of methodology: G.P. Leung, T. Feng, D.A. Ruddy, D.D. Stuart
Acquisition of data (provided animals, acquired and managed patients, provided facilities, etc.): G.P. Leung, T. Feng, D.A. Ruddy
Analysis and interpretation of data (e.g., statistical analysis, biostatistics, computational analysis): G.P. Leung, T. Feng, F.D. Sigoillot, F.C. Geyer, M.D. Shirley, J.A. Engelman, M. Jaskelioff, D.D. Stuart
Writing, review, and/or revision of the manuscript: G.P. Leung, F.D. Sigoillot, M.D. Shirley, A.K. Freeman, J.A. Engelman, M. Jaskelioff, D.D. Stuart
Administrative, technical, or material support (i.e., reporting or organizing data, constructing databases): G.P. Leung, D. Rakiec, M. Jaskelioff, D.D. Stuart
Study supervision: A.K. Freeman, M. Jaskelioff, D.D. Stuart

Acknowledgments

We thank M. Crowe and E.R. McDonald for helpful discussion and A. Ho, J. Reece-Hoyes, and A. Farsidjani for technical assistance.

The costs of publication of this article were defrayed in part by the payment of page charges. This article must therefore be hereby marked *advertisement* in accordance with 18 U.S.C. Section 1734 solely to indicate this fact.

Received April 3, 2018; revised July 25, 2018; accepted August 30, 2018; published first September 10, 2018.

References

1. Davies H, Bignell GR, Cox C, Stephens P, Edkins S, Clegg S, et al. Mutations of the BRAF gene in human cancer. Nature 2002;417:949–54.
2. Cancer Genome Atlas Network. Genomic classification of cutaneous melanoma. Cell 2015;161:1681–96.
3. Hodis E, Watson IR, Kryukov GV, Arold ST, Imielinski M, Theurillat JP, et al. A landscape of driver mutations in melanoma. Cell 2012;150:251–63.
4. Chapman PB, Hauschild A, Robert C, Haanen JB, Ascierto P, Larkin J, et al. Improved survival with vemurafenib in melanoma with BRAF V600E mutation. N Engl J Med 2011;364:2507–16.
5. Hauschild A, Grob JJ, Demidov LV, Jouary T, Gutzmer R, Millward M, et al. Dabrafenib in BRAF-mutated metastatic melanoma: a multicentre, open-label, phase 3 randomised controlled trial. Lancet 2012;380:358–65.
6. Emery CM, Vijayendran KG, Zipser MC, Sawyer AM, Niu L, Kim JJ, et al. MEK1 mutations confer resistance to MEK and B-RAF inhibition. Proc Natl Acad Sci U S A 2009;106:20411–6.
7. Nazarian R, Shi H, Wang Q, Kong X, Koya RC, Lee H, et al. Melanomas acquire resistance to B-RAF(V600E) inhibition by RTK or N-RAS upregulation. Nature 2010;468:973–7.
8. Shi H, Hugo W, Kong X, Hong A, Koya RC, Moriceau G, et al. Acquired resistance and clonal evolution in melanoma during BRAF inhibitor therapy. Cancer Discov 2014;4:80–93.
9. Shi H, Moriceau G, Kong X, Koya RC, Nazarian R, Pupo GM, et al. Preexisting MEK1 exon 3 mutations in V600E/KBRAF melanomas do not confer resistance to BRAF inhibitors. Cancer Discov 2012;2:414–24.
10. Wagle N, Emery C, Davis MJ, Sawyer A, Pochanard P, Kehoe SM, et al. Dissecting therapeutic resistance to RAF inhibition in melanoma by tumor genomic profiling. J Clin Oncol 2011;29:3085–96.
11. Wang H, Daouti S, Li WH, Wen Y, Rizzo C, Higgins B, et al. Identification of the MEK1(F129L) activating mutation as a potential mechanism of acquired resistance to MEK inhibition in human cancers carrying the B-RafV600E mutation. Cancer Res 2011;71:5535–45.
12. Corcoran RB, Dias-Santagata D, Bergethon K, Iafrate AJ, Settleman J, Engelman JA. BRAF gene amplification can promote acquired resistance to MEK inhibitors in cancer cells harboring the BRAF V600E mutation. Sci Signal 2010;3:ra84.
13. Poulikakos PI, Persaud Y, Janakiraman M, Kong X, Ng C, Moriceau G, et al. RAF inhibitor resistance is mediated by dimerization of aberrantly spliced BRAF(V600E). Nature 2011;480:387–90.
14. Shi H, Moriceau G, Kong X, Lee MK, Lee H, Koya RC, et al. Melanoma whole-exome sequencing identifies (V600E)B-RAF amplification-mediated acquired B-RAF inhibitor resistance. Nat Commun 2012;3:724.
15. Das Thakur M, Salangsang F, Landman AS, Sellers WR, Pryer NK, Levesque MP, et al. Modelling vemurafenib resistance in melanoma reveals a strategy to forestall drug resistance. Nature 2013;494:251–5.
16. Hong A, Moriceau G, Sun L, Lomeli S, Piva M, Damoiseaux R, et al. Exploiting drug addiction mechanisms to select against MAPKi-resistant melanoma. Cancer Discov 2018;8:74–93.
17. Kong X, Kuilman T, Shahrabi A, Boshuizen J, Kemper K, Song JY, et al. Cancer drug addiction is relayed by an ERK2-dependent phenotype switch. Nature 2017;550:270–4.
18. Moriceau G, Hugo W, Hong A, Shi H, Kong X, Yu CC, et al. Tunable-combinatorial mechanisms of acquired resistance limit the efficacy of BRAF/MEK cotargeting but result in melanoma drug addiction. Cancer Cell 2015;27:240–56.
19. Barretina J, Caponigro G, Stransky N, Venkatesan K, Margolin AA, Kim S, et al. The Cancer Cell Line Encyclopedia enables predictive modelling of anticancer drug sensitivity. Nature 2012;483:603–7.
20. Hoffman GR, Rahal R, Buxton F, Xiang K, McAllister G, Frias E, et al. Functional epigenetics approach identifies BRM/SMARCA2 as a critical synthetic lethal target in BRG1-deficient cancers. Proc Natl Acad Sci U S A 2014;111:3128–33.
21. McDonald ER III, de Weck A, Schlabach MR, Billy E, Mavrakis KJ, Hoffman GR, et al. Project DRIVE: a compendium of cancer dependencies and synthetic lethal relationships uncovered by large-scale, deep RNAi screening. Cell 2017;170:577–92.
22. Bhang HE, Ruddy DA, Krishnamurthy Radhakrishna V, Caushi JX, Zhao R, Hims MM, et al. Studying clonal dynamics in response to cancer therapy using high-complexity barcoding. Nat Med 2015;21:440–8.
23. Mootha VK, Lindgren CM, Eriksson KF, Subramanian A, Sihag S, Lehar J, et al. PGC-1alpha-responsive genes involved in oxidative phosphorylation are coordinately downregulated in human diabetes. Nat Genet 2003;34:267–73.
24. Subramanian A, Tamayo P, Mootha VK, Mukherjee S, Ebert BL, Gillette MA, et al. Gene set enrichment analysis: a knowledge-based approach for interpreting genome-wide expression profiles. Proc Natl Acad Sci U S A 2005;102:15545–50.
25. Huang da W, Sherman BT, Lempicki RA. Bioinformatics enrichment tools: paths toward the comprehensive functional analysis of large gene lists. Nucleic Acids Res 2009;37:1–13.
26. Huang da W, Sherman BT, Lempicki RA. Systematic and integrative analysis of large gene lists using DAVID bioinformatics resources. Nat Protoc 2009;4:44–57.
27. Roskoski R. ERK1/2 MAP kinases: structure, function, and regulation. Pharmacol Res 2012;66:105–43.
28. Elmore S. Apoptosis: a review of programmed cell death. Toxicol Pathol 2007;35:495–516.
29. Mizushima N. Autophagy: process and function. Genes Dev 2007;21:2861–73.
30. Sulli G, Di Micco R, d'Adda di Fagagna F. Crosstalk between chromatin state and DNA damage response in cellular senescence and cancer. Nat Rev Cancer 2012;12:709–20.
31. Sano R, Reed JC. ER stress-induced cell death mechanisms. Biochim Biophys Acta 2013;1833:3460–70.
32. Cuenda A, Rousseau S. p38 MAP-kinases pathway regulation, function and role in human diseases. Biochim Biophys Acta 2007;1773:1358–75.
33. Hatzivassiliou G, Song K, Yen I, Brandhuber BJ, Anderson DJ, Alvarado R, et al. RAF inhibitors prime wild-type RAF to activate the MAPK pathway and enhance growth. Nature 2010;464:431–5.
34. Heidorn SJ, Milagre C, Whittaker S, Nourry A, Niculescu-Duvas I, Dhomen N, et al. Kinase-dead BRAF and oncogenic RAS cooperate to drive tumor progression through CRAF. Cell 2010;140:209–21.
35. Poulikakos PI, Zhang C, Bollag G, Shokat KM, Rosen N. RAF inhibitors transactivate RAF dimers and ERK signalling in cells with wild-type BRAF. Nature 2010;464:427–30.
36. Su F, Viros A, Milagre C, Trunzer K, Bollag G, Spleiss O, et al. RAS Mutations in cutaneous squamous-cell carcinomas in patients treated with BRAF inhibitors. N Engl J Med 2012;366:207.
37. Hong SK, Yoon S, Moelling C, Arthan D, Park JI. Noncatalytic function of ERK1/2 can promote Raf/MEK/ERK-mediated growth arrest signaling. J Biol Chem 2009;284:33006–18.
38. Seoane J, Gomis RR. TGF-beta family signaling in tumor suppression and cancer progression. Cold Spring Harb Perspect Biol 2017;9:pii: a022277.
39. Cox AD, Fesik SW, Kimmelman AC, Luo J, Der CJ. Drugging the undruggable RAS: mission possible? Nat Rev Drug Discov 2014;13:828–51.
40. Lake D, Corrêa SA, Müller J. Negative feedback regulation of the ERK1/2 MAPK pathway. Cell Mol Life Sci 2016;73:4397–413.
41. Pratilas CA, Taylor BS, Ye Q, Viale A, Sander C, Solit DB, et al. (V600E)BRAF is associated with disabled feedback inhibition of RAF-MEK signaling and elevated transcriptional output of the pathway. Proc Natl Acad Sci U S A 2009;106:4519–24.
42. Goetz EM, Ghandi M, Treacy DJ, Wagle N, Garraway LA. ERK mutations confer resistance to mitogen-activated protein kinase pathway inhibitors. Cancer Res 2014;74:7079–89.
43. Maddodi N, Huang W, Havighurst T, Kim K, Longley BJ, Setaluri V. Induction of autophagy and inhibition of melanoma growth in vitro and in vivo by hyperactivation of oncogenic BRAF. J Invest Dermatol 2010;130:1657–67.
44. Unni AM, Lockwood WW, Zejnullahu K, Lee-Lin SQ, Varmus H. Evidence that synthetic lethality underlies the mutual exclusivity of oncogenic KRAS and EGFR mutations in lung adenocarcinoma. ELife 2015;4:e06907.
45. Suda K, Tomizawa K, Osada H, Maehara Y, Yatabe Y, Sekido Y, et al. Conversion from the "oncogene addiction" to "drug addiction" by intensive inhibition of the EGFR and MET in lung cancer with activating EGFR mutation. Lung Cancer 2011;76:292–9.
46. Amin AD, Rajan SS, Liang WS, Pongtornpipat P, Groysman MJ, Tapia EO, et al. Evidence suggesting that discontinuous dosing of ALK kinase inhibitors may prolong control of ALK+ tumors. Cancer Res 2015;75:2916–27.
47. Gorgoulis VG, Halazonetis TD. Oncogene-induced senescence: the bright and dark side of the response. Curr Opin Cell Biol 2010;22:816–27.